THE AMERICAN SOCIETY OF MECHANICAL ENGINEERS
345 E. 47 St., New York, N.Y. 10017

92-WA/DSC-10

A Geometric Representation of Root Sensitivity

T. R. KURFESS and M. L. NAGURKA
Department of Mechanical Engineering
Carnegie Mellon University
Pittsburgh, PA 15213

In this paper, we present a geometric method for representing the classical root sensitivity function of linear time–invariant dynamic systems. The method employs specialized eigenvalue plots that expand the information presented in the root locus plot in a manner that permits determination by inspection of both the real and imaginary components of the root sensitivity function. We observe relationships between root sensitivity and eigenvalue geometry that do not appear to be reported in the literature and hold important implications for control system design and analysis.

THE ROOT SENSITIVITY FUNCTION

In classical control theory the root sensitivity, S_p, is defined as the relative change in the system roots or eigenvalues, λ_i (i = 1,..., n), with respect to a system parameter, p. Most often, the parameter analyzed is the forward proportional controller gain, k. The root sensitivity with respect to gain is given by

$$S_k = \frac{d\lambda(k) / \lambda(k)}{dk / k} = \frac{d\lambda(k)}{dk} \frac{k}{\lambda(k)} \qquad (1)$$

Since the eigenvalues may occur as complex conjugate pairs, S_k may be complex.

Equation (1) is often introduced in determining the break points of the Evans root locus plot for single-input single-output systems. At the break points, S_k becomes infinite as at least two of the n system eigenvalues undergo a transition from the real domain to the complex domain or vice versa. This transition causes an abrupt change in the relation between the eigenvalue angle $\angle\lambda$ and gain k yielding an infinite eigenvalue derivative with respect to gain (Ogata, 1990).

The root sensitivity function S_k is a measure of the effect of parameter variations on the eigenvalues. It is important in light of one of the key objectives of feedback control theory to reduce system sensitivity to variations in system parameters. For example, the control system of a robot should be relatively insensitive to the payload carried by the arm for the recommended payload range. If the robot's performance is sensitive to payload variations, then the control system is not robust and performance is difficult to guarantee. In this case, S_m, where m is the payload mass, should be relatively small over the operational range of m. Such considerations are critical if control designers are to develop high performance, robust, closed-loop systems.

In this paper, we present a geometric technique for root sensitivity. The technique relies on a set of plots called gain plots (Kurfess and Nagurka, 1991a) that are an alternate visualization of the Evans root locus plot. In particular, we prove that the slopes of the gain plots are directly related to the real and imaginary components of the sensitivity function. Two examples are presented demonstrating the insight gained via this geometric perspective on the sensitivity function, and its utility in control system design and analysis.

Presented at the Winter Annual Meeting
November 8-13, 1992—Anaheim, CA

ROOT SENSITIVITY ANALYSIS

In this section, we derive the complex root sensitivity function by employing a polar representation of the eigenvalues in the complex plane. We proceed by positing three assumptions: *(i)* the systems analyzed are lumped parameter, linear time–invariant (LTI) systems; *(ii)* there are no eigenvalues at the origin of the s-plane, *i.e.*,

$$\lambda_i \neq 0 \ , \ \forall i = 1, ..., n \tag{2}$$

(although the eigenvalues may be arbitrarily close to the origin singularity); and *(iii)* the forward scalar gain, k, is real and positive, *i.e.*, $k \in \Re$, $k > 0$. Based on these assumptions, we draw the following observations: the real component of the sensitivity function is given by

$$\mathrm{Re}\{S_k\} = \frac{d\ln|\lambda(k)|}{d\ln(k)} \tag{3}$$

and the imaginary component of the sensitivity function is given by

$$\mathrm{Im}\{S_k\} = \frac{d\angle\lambda(k)}{d\ln(k)} \tag{4}$$

where $\angle\lambda$ is the eigenvalue angle.

These observations may be proven as follows. Equation (1) may be rewritten (Horowitz, 1963; Kuo, 1991) in terms of the derivatives of natural logarithms as

$$S_k = \frac{d\ln(\lambda(k))}{d\ln(k)} \tag{5}$$

The natural logarithm of the complex value, λ, is equal to the sum of the logarithm of the magnitude of λ and the angle of λ multiplied by $j = \sqrt{-1}$. Thus, equation (5) becomes

$$S_k = \frac{d[\ln|\lambda(k)| + j\angle\lambda(k)]}{d\ln(k)} \tag{6}$$

Since j is a constant, equation (6) may be rewritten as

$$S_k = \frac{d\ln|\lambda(k)|}{d\ln(k)} + j\frac{d\angle\lambda(k)}{d\ln(k)} \tag{7}$$

The complex root sensitivity function is now expressed with distinct real and imaginary components employing the polar form of the eigenvalues. It follows from assumption *(ii)* that ln(k) is real. (In general, most parameters studied are real and this proof is sufficient. If, however, the parameter analyzed is complex, it is a straightforward task to extend the above analysis.)

The proof is completed by taking the real and imaginary components of equation (7), yielding equations (3) and (4). It is interesting to note that the Cartesian representation of S_k is related to the polar representation of λ_i.

GEOMETRIC RELATIONS TO GAIN PLOTS

The gain plots are an alternate graphical representation of the Evans root locus plot (Kurfess and Nagurka, 1991a). They explicitly graph the eigenvalue magnitude *vs.* gain in a magnitude gain plot and the eigenvalue angle *vs.* gain in an angle gain plot. The magnitude gain plot employs a log–log scale whereas the angle gain plot uses a semi–log scale (with the logarithms being base 10.) Although we use gain as the variable of interest, it should be noted that any parameter may be used in the geometric analysis.

We next make the observation that the slope of the magnitude gain plot is the real component of S_k. The magnitude gain plot slope, M_m, is

$$M_m = \frac{d\ \log(|\lambda(k)|)}{d\ \log\ (k)} \tag{8}$$

which may be rewritten as

$$M_m = \frac{d\,[\log(e)\ln(|\lambda(k)|)]}{d\,[\log(e)\ln(k)]} = \frac{d\ \ln(|\lambda(k)|)}{d\ \ln\ (k)} \tag{9}$$

corresponding to equation (3).

Furthermore, the slope of the angle gain plot is linearly related to the imaginary component of S_k by the constant, $(\log(e))^{-1}$. The angle gain plot slope, M_a, is

$$M_a = \frac{d\ \angle\lambda(k)}{d\ \log\ (k)} \tag{10}$$

which may be rewritten as

$$M_a = \frac{d\ \angle\lambda(k)}{d\,[\log(e)\ln(k)]} = \frac{1}{\log(e)}\frac{d\ \angle\lambda(k)}{d\ \ln\ (k)} \tag{11}$$

and hence M_a is proportionally related to equation (4) by $(\log(e))^{-1}$.

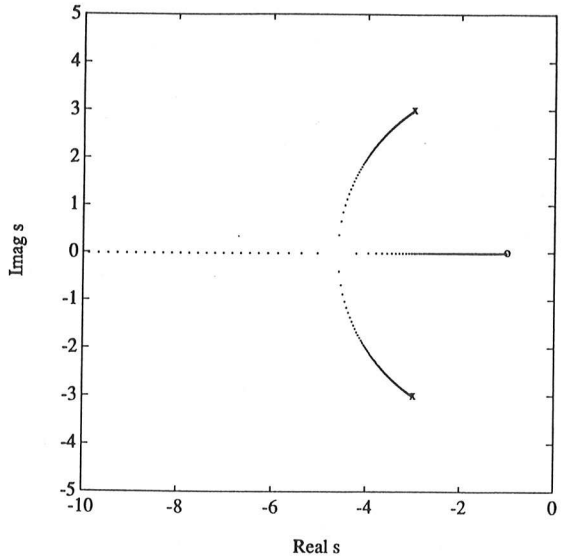

Figure 1. Root Locus Plot for Equation (14)

EXAMPLES

In this section we demonstrate the graphical method of determining the root sensitivity function. The first example employs a closed-loop system in which the forward loop gain is varied. The goal of this example is to introduce the proposed graphical view of root sensitivity; the example is purposely designed to be straightforward and intuitive.

The second example involves a system using positive modal feedback (Sardar and Paul, 1991). We use this more complicated system to demonstrate the determination of the root sensitivity function with respect to a system parameter, namely stiffness. The example demonstrates the utility of extending the root locus to system variables other than the control gain, enabling the control designer to conduct parametric sensitivity studies when designing and analyzing control systems.

Traditional PD Controller Example

This example considers the plant

$$g_p(s) = \frac{1}{s^2 + 6s + 18} \tag{12}$$

with a PD compensator

$$g_c(s) = k\,(s + 1) \tag{13}$$

giving the loop–transmission transfer function

$$g(s) = g_p(s)\, g_c(s) = \frac{k\,(s + 1)}{s^2 + 6s + 18} \tag{14}$$

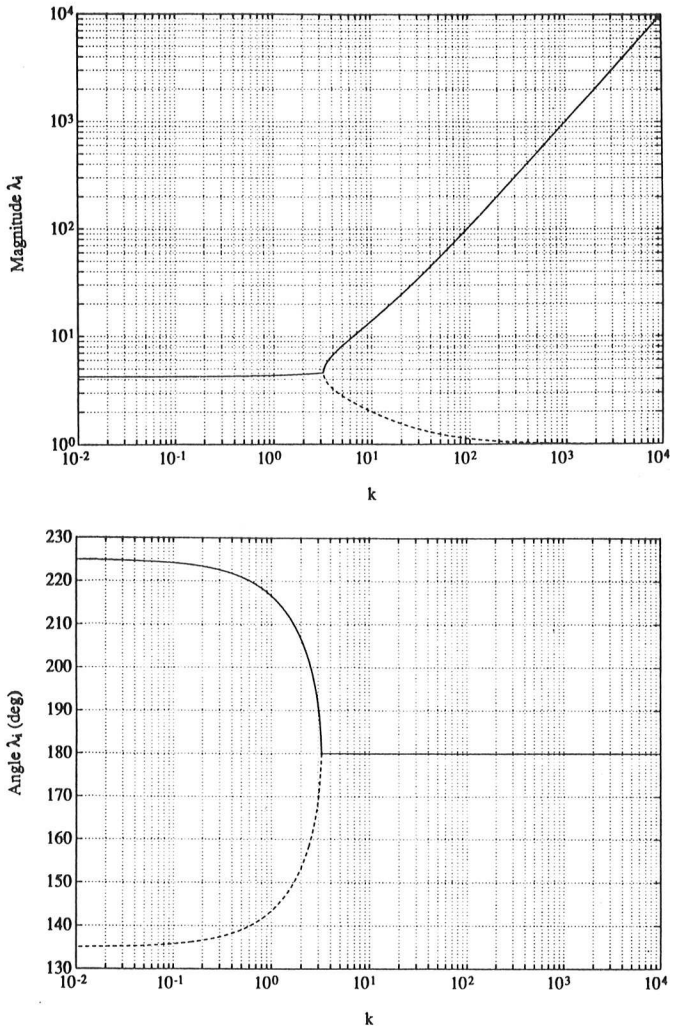

Figure 2. (a) Magnitude and (b) Angle Gain Plots for Equation (14)

The root locus plot of Figure 1 portrays the effect of varying gain k. An alternate visualization is shown in the magnitude gain plot and angle gain plot of Figures 2a,b, respectively. These figures show that the eigenvalues are either completely real or are complex conjugate values. The real and imaginary components of S_k are plotted as functions of gain in Figures 3a,b. These are determined from the slopes of the magnitude gain plot and angle gain plot, respectively.

Figures 2a,b and 3a,b show that the break point occurs at $k_{bp} \cong 3.21$. In particular, Figures 3a,b highlight the infinite values of the real and imaginary eigenvalue components at k_{bp}. Below k_{bp} the closed–loop eigenvalues follow a circular trajectory about the point s = –1 as demonstrated in Figure 1.

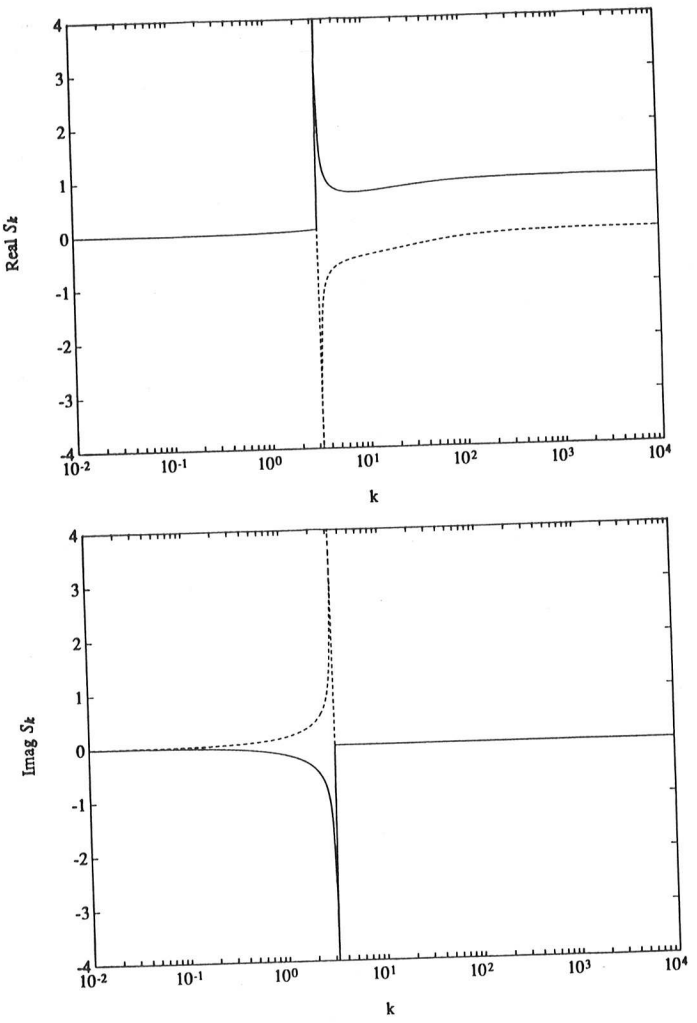

Figure 3. (a) Real and (b) Imaginary Component of S_k for Equation (14)

Figures 2a and 3a show that the eigenvalues have coincident trajectories below k_{bp}. Above k_{bp} one eigenvalue migrates to the finite transmission zero at s=–1 while the other eigenvalue migrates to the infinite zero at $-\infty$. At high gains the real components of S_k are zero and one, respectively (Kurfess and Nagurka, 1991b). Thus, at high gains the finite transmission zero is desensitized from k, and there is a unity magnitude relation between k and the finite eigenvalue. In contrast to Figures 2a and 3a, Figures 2b and 3b show multi–valued eigenvalue trajectories above k_{bp} and coincident trajectories below k_{bp}. This is expected since the eigenvalues are either purely real or complex conjugates. Finally, since the eigenvalues are purely real above k_{bp}, the imaginary component of S_k is zero for $k > k_{bp}$.

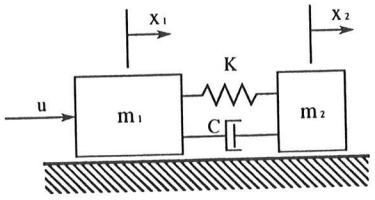

Parameter Values
(Sardar and Paul, 1991)

K = 14,400 N/m
C = 1.2 N-s/m
m_1 = 20 kg
m_2 = 2 kg

Figure 4. Lumped Parameter System Model

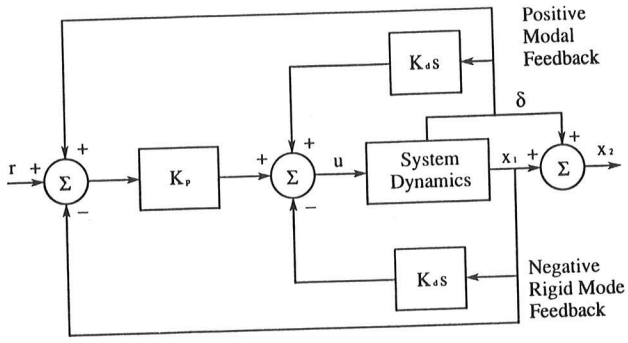

Figure 5. Block Diagram with PD Control and Positive Modal Feedback

Positive Modal Feedback Example

Sardar and Paul (1991) considered the application of positive modal feedback to the dynamic system, shown in Figure 4, representing a lumped parameter structural model. The block diagram of the positive modal feedback is shown in Figure 5. The transfer function between the actual and desired position (R(s)) is

$$\frac{X_2(s)}{R(s)} = \frac{K_p(Cs + K)}{b_4 s^4 + b_3 s^3 + b_2 s^2 + b_1 s + b_0} \tag{15}$$

where

$$b_4 = m_1 m_2 \tag{16}$$

$$b_3 = 2m_2 K_d + (m_1 + m_2)C \tag{17}$$

$$b_2 = 2m_2 K_p + (m_1 + m_2)K + K_d C \tag{18}$$

$$b_1 = K_p C + K_d K \tag{19}$$

$$b_0 = K_p K \tag{20}$$

where K_p is the proportional gain and K_d is the derivative gain. The term, δ, in Figure 5 is the relative vibration of the masses given by

$$\delta = x_2 - x_1 \tag{21}$$

In their work, Sardar and Paul assumed a value of $K_d = 200$, and varied the value of K_p to generate root

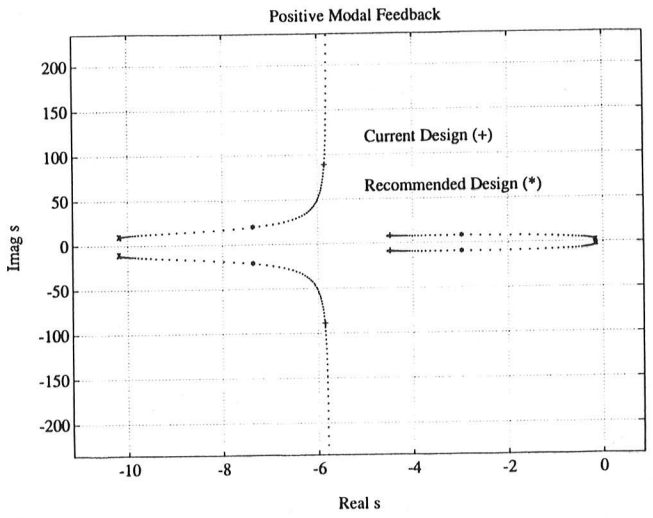

Figure 6. Root Locus Plot for Equation (15)

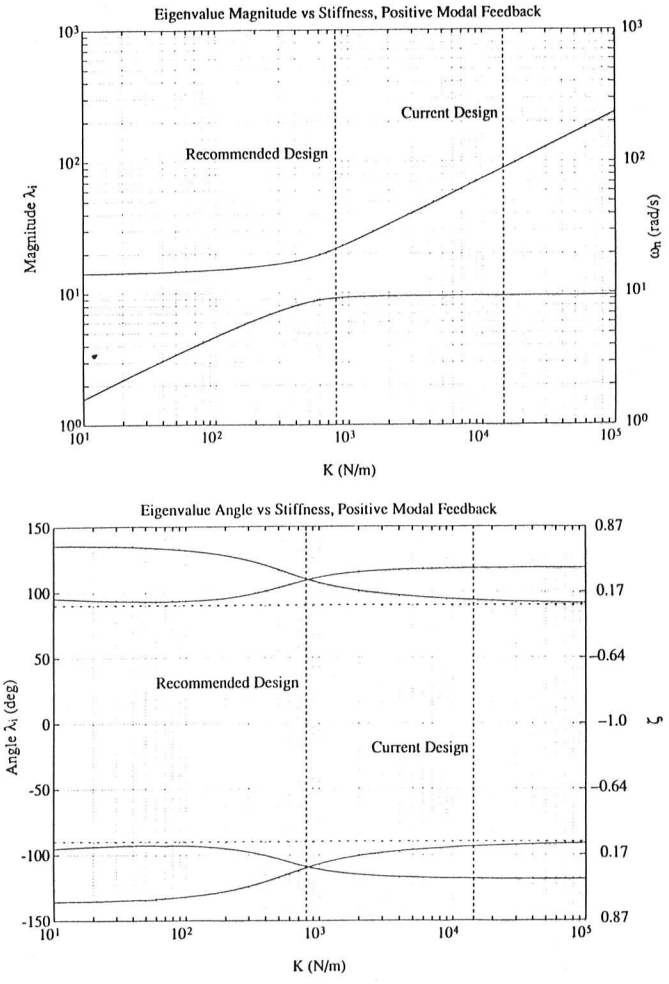

Figure 7. (a) Magnitude and (b) Angle Gain Plots for Equation (15)

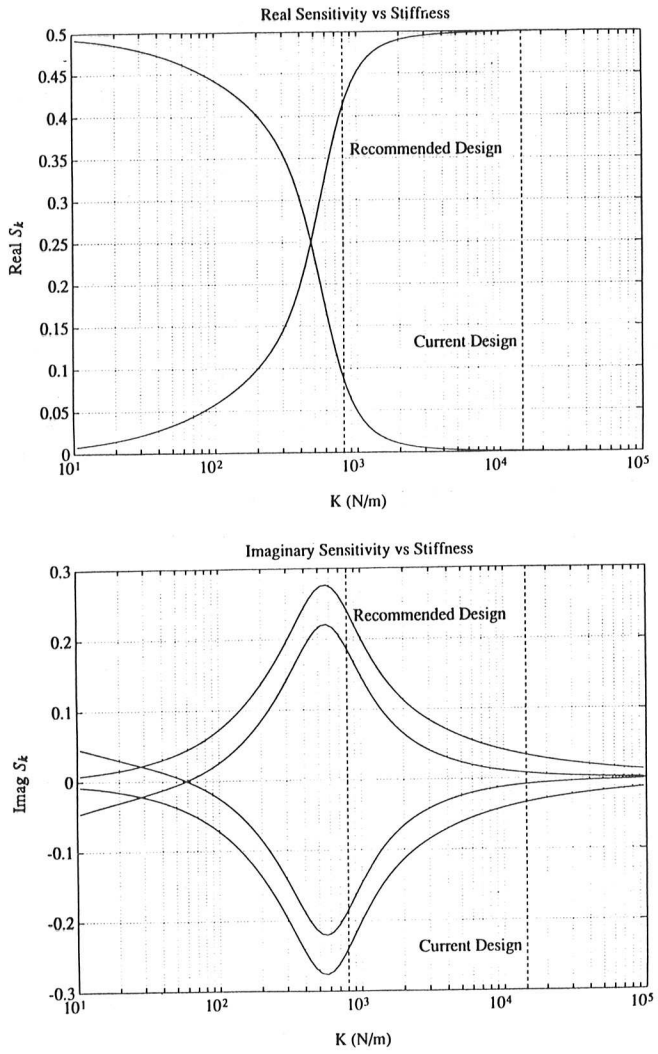

Figure 8. (a) Real and (b) Imaginary Component of S_k for Equation (15)

locus plots. It is our objective to pick a value of K_p and then conduct a sensitivity analysis of the closed-loop system with respect to the spring stiffness, K. We use a value of $K_p = 2000$, yielding a stable system, and sweep K through a large range (including the value used by Sardar and Paul, K = 14400 N/m). Figure 6 is the root locus for the closed-loop system as K is varied in the range $10^1 \le K \le 10^5$. (Note that the root locus axes are *not* the same scale.) Figures 7a,b and 8a,b are the gain plots and sensitivity plots, respectively, for the system. In the gain plots, natural frequency and damping ratio vertical axes have been added to aid in the analysis.

From these figures, several interesting features

are available. First, the entire range of K corresponds a closed-loop stable system. The design does, however, place a set of high frequency poles near the imaginary axis. These poles represent the mode of the system. The designer cannot ignore these poles since they do not decay fast enough, with respect to the other pole pair, to invoke the dominant pole theory. The design may indeed meet specifications; however, let us assume that we would like a bit more damping. There is the possibility of reducing the stiffness, K, which results in increasing the damping, ζ. By inspection from the angle gain plot, the value of K that results in the highest damping for both pole pairs is approximately K=870 N/m. This is where the damping ratio for both sets is approximately equal. At K=870 N/m, we can read the natural frequency for each pole pair from the magnitude gain plot to be 9 and 20 rad/sec, respectively.

We may now examine the sensitivity plots to see if our design is robust to variations in K. The plots indicate that the design is fairly robust to stiffness variations. The real part of the sensitivity function indicates sensitivities of 0.07 and 0.42 for the lower and higher frequency pole pairs, respectively. This translates to the fact that a 10% increase in K will yield a 0.7% increase in the low frequency pole pair's natural frequency, and a 4.2% variation in the natural frequency of the high frequency poles. The values of the imaginary part of the root sensitivity function are approximately 0.24 and 0.18 for the higher and lower frequency pole pairs, respectively. Again, this translates directly to the rate at which the pole angles (and thus damping) change as a function of K.

From both of these plots, the control designer may observe that the chosen design does not generate a highly sensitive system. Furthermore, higher stiffnesses relate to smaller imaginary components of the sensitivity function. For higher stiffnesses, the real part of the root sensitivity for the higher frequency pole pair increases asymptotically to 0.5, while the lower frequency pair approaches zero. Several design insights may be garnered from these plots. First, stiffnesses of 500 may not be desirable if low damping variations are critical. Figure 8b demonstrates that the imaginary part of the sensitivity function is maximum at that range. However, at a K of approximately 400, the real part of the root sensitivity function is equal for both pole pairs. Therefore, if the radial pole motion of both pairs is to be minimized, a stiffness of 400 may be considered. Finally at high stiffnesses such as 10^4, the root sensitivity function is relatively flat. Thus, stiffness variations at these higher values should result in predictable changes in pole locations.

CLOSING

The concept of root sensitivity in classical controls is often introduced to emphasize the high "sensitivity" of eigenvalues with respect to a system parameter such as gain near the break–points. Normally, the root sensitivity function is not discussed as a complex quantity in control system analysis and design. Here, we have derived and demonstrated a powerful means to visualize the root sensitivity function via the gain plots. The slopes of the gain plots provide a direct measure of the real and imaginary components of the root sensitivity, and are available by inspection. The use of the gain plots in conjunction with other traditional graphical techniques offers the control system designer important information for selection of appropriate system parameters.

ACKNOWLEDGEMENT

This work was funded in part by the National Science Foundation under grant DDM-9015643. Any opinions, findings and conclusions or recommendations are those of the authors and do not necessarily reflect the views of the National Science Foundation. The authors would also like to thank Mr. Ssu-Kuei Wang for his help, and for his enthusiasm of gain plots.

REFERENCES

I.M. Horowitz, 1963, Synthesis of Feedback Systems, Academic Press, New York.

B.C. Kuo, 1991, Automatic Control Systems, Fifth Edition, Prentice Hall, Englewood Cliffs, NJ.

T. R. Kurfess and M. L. Nagurka, 1991a, "Understanding the Root Locus Using Gain Plots," IEEE Control Systems Magazine, Vol. 11, No. 5, pp. 37–40.

T. R. Kurfess and M. L. Nagurka, 1991b, "A Geometric Paradigm Exposing High Gain Root Sensitivity of Single–Input Single–Output Systems," Technical Report #EDRC 24–60–91, Engineering Design Research Center, Pittsburgh, PA.

K. Ogata, 1990, Modern Control Engineering, Second Edition, Prentice–Hall, Englewood Cliffs, NJ.

H. M. Sardar and F. W. Paul, 1991 "Controlling Structural Vibrations Using Positive Modal Feedback," ASME Symposium Volume DSC-Vol. 31, pp 113-120.